

Chameleon attractors in a turbulent flow

Tommaso Alberti*

*INAF-Istituto di Astrofisica e Planetologia Spaziali,
via del Fosso del Cavaliere 100, 00133 Rome, Italy*

Francois Daviaud

CEA, IRAMIS, SPEC, CNRS URA 2464, SPHYNX, 91191 Gif-sur-Yvette, France

Reik V. Donner

*Department of Water, Environment, Construction and Safety,
Magdeburg–Stendal University of Applied Sciences,
Breitscheidstraße 2, 39114 Magdeburg, Germany and
Research Department I – Earth System Analysis,
Potsdam Institute for Climate Impact Research (PIK) – Member of
the Leibniz Association, Telegrafenberg A31, 14473 Potsdam, Germany*

Berengere Dubrulle

SPEC, CEA, CNRS, Université Paris-Saclay, F-91191 CEA Saclay, Gif-sur-Yvette, France

Davide Faranda

*Laboratoire des Sciences du Climat et de l'Environnement,
CEA Saclay l'Orme des Merisiers, UMR 8212 CEA-CNRS-UVSQ,
Université Paris-Saclay & IPSL, 91191, Gif-sur-Yvette, France.
London Mathematical Laboratory, 8 Margravine Gardens, London, W6 8RH, UK. and
LMD/IPSL, Ecole Normale Supérieure, PSL research University, 75005, Paris, France.*

Valerio Lucarini

*Department of Mathematics and Statistics, University of Reading, Reading, UK. and
Centre for the Mathematics of Planet Earth, University of Reading, RG6 6AX, Reading, UK.*

(Dated: December 21, 2021)

Turbulent flows in geophysical systems often present rich dynamics originating from non-trivial energy fluxes in scale space, non-stationary forcings and geometrical constraints. This complexity appears via non-hyperbolic chaos, randomness, state-dependent persistence and predictability. All these features have prevented a full characterization of the underlying turbulent (stochastic) attractor, which will be the key object to unpin this complexity. Here we use a novel formalism to map unstable fixed points to singularities of turbulent flows and to trace the evolution of their structural characteristics when moving from small to large scales and vice versa, providing a full characterization of the attractor. We demonstrate that the properties of the dynamically invariant objects depend on the scale we are focusing on. Given the changing nature of such attractors in time, space and scale spaces, we term them *chameleon* attractors.

A glass of water consists of about $10N_A$ water molecules (with $N_A = 6.022 \times 10^{23} \text{ mol}^{-1}$ being the Avogadro number), which obey collisional dynamics that can be derived from quantum mechanics equations. Yet, nobody will attempt to compute the dynamics of the water inside the glass by integrating the coupled equations for the water molecules because it would mean taking track of so many degrees of freedom that it would saturate any computer memory, however large [1]. Instead, one will rather use a coarse-grained set of equations, the Navier-Stokes equations (NSE), derived as the macroscopic dynamic laws resulting from the mesoscopic Boltzmann equation [2]. The NSE describe accurately the dynamics of averaged quantities over spatial scales that are

much larger than the mean free path length of the water molecules [3]. The number of Fourier modes needed to simulate the NSE on a regular grid can roughly be estimated as $(L/\eta)^3$, where L is the largest scale of the system, and η the Kolmogorov scale, at which the input energy is dissipated by viscosity [4]. In our glass of water slowly stirred by a spoon, where laminar flow is realized, the effective number of degrees of freedom then reduces to just a few. By contrast, when we consider large-scale turbulent motions, such as in most geophysical flows, even the most powerful computer on Earth falls very short from being able to describe accurately the behavior of the NSE at all relevant scales of motions. Hence, there is a need for deriving approximate equations able to describe accurately the dynamics on a reduced range of spatial and temporal scales [5] and to develop accurate yet efficient parametrizations for describing the impact

* tommaso.alberti@inaf.it

of the unresolved scales of motions on those of interest [6, 7].

One way to approach the description of fluid flows containing a large number of scales is via a global statistical analysis. This was the main aim of the multifractal formalism developed by Parisi and Frisch [8]. It is basically framed in the large deviation theory [9, 10], contrasting the usual idea, coming from critical phenomena, that only a countable set of scaling exponents are relevant for a complete characterization of the statistical features of fluid flows. Thus, an infinite set of exponents, each belonging to a given fractal set, is required [11]. The probability of observing a singularity of scaling exponent h depends on a function $C(h)$ which can be interpreted as the co-dimension of the fractal set [12]. The multifractal spectrum is then derived as $D(h) = D - C(h)$, with D being the space dimension [13]. The multifractal theory assumes that the velocity has a local scale-invariance, i.e., $\delta v_\ell \sim \ell^h$, to assess the statistical properties of fluids in a robust way with respect to noise and limited statistics [14]. Since its development experimental measurements of the velocity field in fluids have proved to be compatible with this multifractal picture, with the most probable scaling exponent $h \sim 1/3$, as predicted by the Kolmogorov theory [4, 15–19]. However, the multifractal theory only provides global information on the scale-dependent properties of fluids via the probability of occurrence of a given scaling exponent. Moreover, a direct computation of the multifractal spectrum from the NSE is not possible [20], although it would be helpful to explore the local statistics of velocity field fluctuations [1].

Since the pioneering work of Ed Lorenz [21], a lot of attention has been paid to dissipative chaotic dynamical systems, with a close connection between turbulence and chaos as proposed by Ruelle and Takens [22]. Indeed, three-dimensional viscous fluids, as described via the NSE, conform to this class of systems, being characterized by strange attractors, i.e., phase-space states toward which the system evolves for a wide range of initial conditions resulting from a series of bifurcations [22]. In this situation, we can theoretically implement a suitable new coarse-graining procedure by projecting the motion onto the basis vectors of the phase-space containing the system’s attractor, resulting in new equations, or computer-accessible numerical simulations.

So far, the search for an attractor underlying turbulent flows in general, and geophysical turbulence in particular has however proved only partially successful. Since the 1990s several studies have suggested that the observed dynamical processes can be associated with the existence of non-hyperbolic strange and possibly stochastic attractors having a dimensionality much lower than the number of degrees of freedom of the system [23, 24]. Non-hyperbolicity manifests itself with the fact that the attractor is heterogeneous in terms of its local properties of persistence and predictability [24, 25]. When considering numerical models, this has important implications

also in terms of error dynamics and efficiency of data assimilation [26].

In this letter, we consider a simple system derived from a turbulent flow by global averaging that removes all space dimensionality, and yet inherits intrinsic properties of the full turbulent system, such as intermittency, bi-stability and the existence of a low-dimensional stochastic attractor [25]. Upon application of new multiscale analysis tools to this system, we demonstrate that its attractor is in fact both scale- and time-dependent, being sensitive to the emergence of an intrinsic timescale solely determined by nonlinear interactions. Because the attractor adapts its geometric and statistical properties dynamically in time with respect to the intrinsic timescale, we call such attractor a “chameleon” attractor.

Data Our data originate from a turbulent von Karman flow, obtained by stirring rapidly water in a vertical cylinder of length $L = 180$ mm and radius $R = 100$ mm. As a result of the forcing, turbulent motions of all temporal and spatial scales develop, and exert onto the two stirring counter-rotating impellers a back-reaction that can be measured through two torque-meters located along their common axis with resulting torques $C_1(t)$ and $C_2(t)$. Hence, these can be seen as large scale quantities that reflect the complex behaviour of the fluid contained in the vessel. Similarly, the instantaneous rotation frequencies $f_1(t)$ and $f_2(t)$ of the two impellers provide a global measure of the large scale circulation that develops under the action of the flux of angular momentum [27–29]. The study of the temporal properties of $f_1(t)$ and $f_2(t)$ as a function of $C_1(t)$ and $C_2(t)$ therefore provides a 1D (time-only) projection of the full 4D (space-time) dynamics of the turbulent flow. Despite this simplification, the resulting system still inherits complex and stochastic properties, and, for special forcing conditions, even develops large-scale circulation cells living on a stochastic attractor [25]. Such a situation is observed under conditions where the two torques C_1 and C_2 applied by the flow onto both impellers are constant, with a typical mean torque $C = \langle (C_1 + C_2)/2 \rangle = 1.68$ Nm. As a result, the two frequencies $f_1(t)$ and $f_2(t)$ fluctuate in time, with a typical mean frequency $f = (f_1 + f_2)/2$ between 4 and 7.5 Hz. The corresponding turbulent flow is then characterized by a Reynolds number $Re = 2\pi R^2 f/\nu \sim 3 \times 10^5$, where ν is the water viscosity. This value significantly exceeds the estimated critical Reynolds number for turbulence onset, $Re_T \approx 3500$.

The time fluctuations of $f_1(t)$ and $f_2(t)$ are not random, but follow an organized pattern that can be detected by using $\gamma = \langle (C_1(t) - C_2(t))/(C_1(t) + C_2(t)) \rangle$ as a control parameter, and $\Theta(t) = (f_1(t) - f_2(t))/(f_1(t) + f_2(t))$ as the order parameter: when $\gamma = 0$ then the top and the bottom impeller are exchangeable, and the turbulent state statistically follows this symmetry. As a result, the top and bottom rotation frequencies are statistically equal such that the variable $\Theta(t) = (f_1(t) - f_2(t))/(f_1(t) + f_2(t))$ fluctuates around zero and characterizes the symmetries of the turbu-

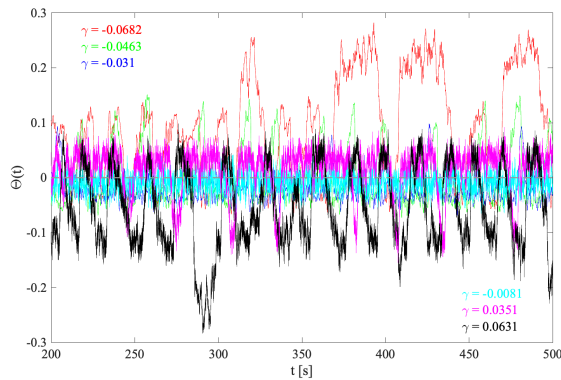


FIG. 1. Behavior of $\Theta(t)$ as function of time for six selected values of $\gamma \in \{-0.0682, -0.0463, -0.031, -0.0081, 0.0351, 0.0631\}$ as reported by red, green, blue, cyan, magenta, and black lines, respectively. The dashed gray lines refer to the value $\Theta(t) = 0$.

lent flow [28, 29]. For values of γ different from zero, the symmetry is broken, and $\Theta(t)$ displays interesting intermittent behaviors, as illustrated in Fig. 1 for six selected values of γ used in this study, i.e., $\gamma \in \{-0.0682, -0.0463, -0.031, -0.0081, 0.0351, 0.0631\}$. Note that in all cases we are imposing modest deviations from the the case of symmetric forcing. As shown in [25], these intermittent behaviors can be globally described by a stochastic strange attractor, whose geometry depends on γ . The global attractor is reconstructed via Takens' embedding method [30] by choosing a fixed delay of $\tau = 20$ time steps (i.e., the value at which the auto-correlation function reduces to 0.5) and an embedding dimension of $m = 3$ [25]. In this way, we move from a univariate time series $\Theta(t)$ to a 3-D multivariate signal $\Theta_\mu(t) = [\Theta(t), \Theta(t - \tau), \Theta(t - 2\tau)]^\dagger = [\Theta_1(t), \Theta_2(t), \Theta_3(t)]^\dagger$ (with \dagger indicating the transposition operator). There is however an additional complexity hidden in this global attractor, that reflects the scale dependent properties of turbulence, as we demonstrate in the following.

Multivariate Empirical Mode Decomposition (MEMD)
To uncover the scale dependence, we first decompose the data into intrinsic modes by using the Multivariate Empirical Mode Decomposition (MEMD). Starting from the multivariate signal $\Theta_\mu(t)$, MEMD exploits its multivariate instantaneous properties to decompose it into a finite number N of multivariate oscillating patterns $\mathbf{C}_{\mu,k}(t)$, called Multivariate Intrinsic Mode Functions (MIMFs), and a monotonic trend $\mathbf{R}_\mu(t)$ as

$$\Theta_\mu(t) = \sum_{k=1}^N \mathbf{C}_{\mu,k}(t) + \mathbf{R}_\mu(t). \quad (1)$$

Each $\mathbf{C}_{\mu,k}(t)$ is a multivariate pattern representative of a peculiar dynamical feature that evolves on a typical mean

timescale τ_k [31]. Thus, the multivariate signal $\Theta_\mu(t)$ is interpreted as a superposition of scale-dependent fluctuations that can be individually investigated for their respective contribution to the collective properties of the whole measurements. A more detailed description is provided in the supplementary material.

Dynamical system metrics We next diagnose the dynamical properties of the instantaneous (in time) and local (in phase-space) states by means of two dynamical systems metrics, the instantaneous local dimension ($0 \leq d < \infty$) and the inverse persistence ($0 \leq \theta \leq 1$). The former is a measure of the active number of degrees of freedom [23], while the latter is a measure of the dynamical stability across the 3-D embedded phase-space [32]. Those instantaneous metrics are obtained by sampling the recurrences of a state ζ and observing that they are distributed according to extreme value theory [23, 33, 34]. Following [35], we can describe the dynamics at scales $\tau' < \tau$ as partial sums of MIMFs

$$\Theta_\mu^\tau(t) = \sum_{k|\tau_k < \tau} \mathbf{C}_{\mu,k}(t) \quad (2)$$

such that we can define a scale-dependent local dimension d_τ and inverse persistence θ_τ by diagnosing the dynamical properties of $\Theta_\mu^\tau(t)$. To do this, we compute both d_τ and θ_τ for reconstructions based on the first k MIMFs as in Eq. (1) until $k \rightarrow N$ for which $(d_\tau, \theta_\tau) \rightarrow (d, \theta)$. Further details can be found in the supplementary material.

Instantaneous scale-dependent dynamical features
Figure 2 shows the results of applying the instantaneous dynamical system metrics to (a) an approximately symmetric case with $\gamma = -0.0081$ and (b) a case with full symmetry breaking at $\gamma = -0.0682$. Other intermediate cases are presented in the supplementary material.

In the symmetric case, one observes that the local indicators are completely scale-invariant, suggesting that the properties of the system do not depend on the scale. The dimension saturates at a value $d \approx 3$, and the inverse persistence is maximal ($\theta = 1$) as expected for an unstructured stochastic system. By contrast, in the non-symmetric case, this scale-invariance is broken. As a result, one observes sudden bursts of local dimensions towards up to $d \approx 6$, localized temporally at frequencies above $f = 6$ Hz, the mean frequency of the system. The inverse persistence displays a markedly different behaviour between scales below and above the mean frequency, with a value close to one for the latter and close to 0 for the former. Since the 3D attractor that we are able to define using $\theta(t)$ is just a projection of a higher-dimensional attractor where the other degrees of freedom are lump in stochastic terms (i.e., at small scales), it is not surprising that we find dimensions larger than 3. As shown in [25], $d > 3$ points towards the existence of an unstable fixed point associated with abrupt changes and hints at the existence of an underlying stochastic attractor. Our scale-dependent results also suggest that, although the flow dynamics involves a wide range of scales, some of them can be described by stochastic theory [36].

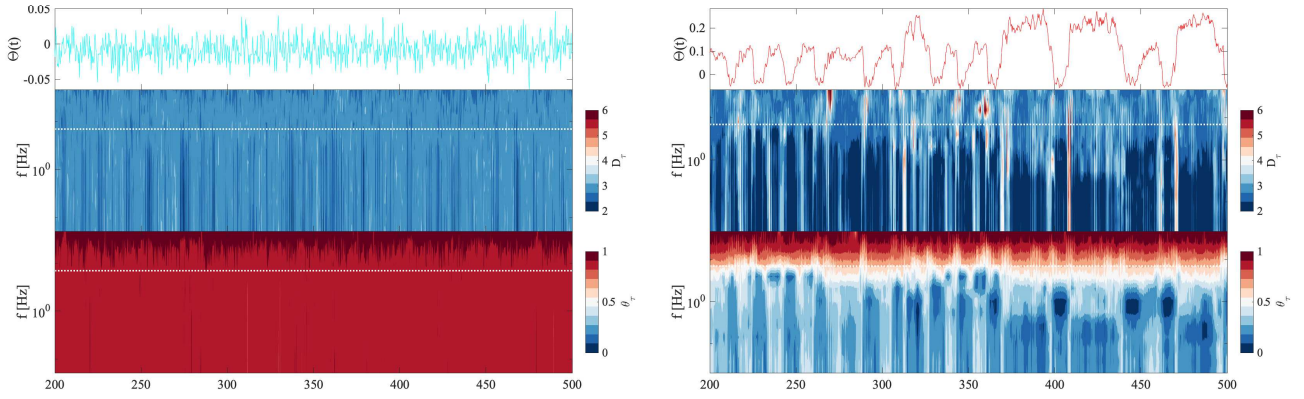


FIG. 2. Temporal behavior of $\Theta(t)$ with γ (upper panel) together with the behavior of the instantaneous dimension d (middle panel) and instantaneous stability θ (lower panel) in the time-frequency domain. Left: $\gamma = -0.0081$, right: $\gamma = -0.0682$.

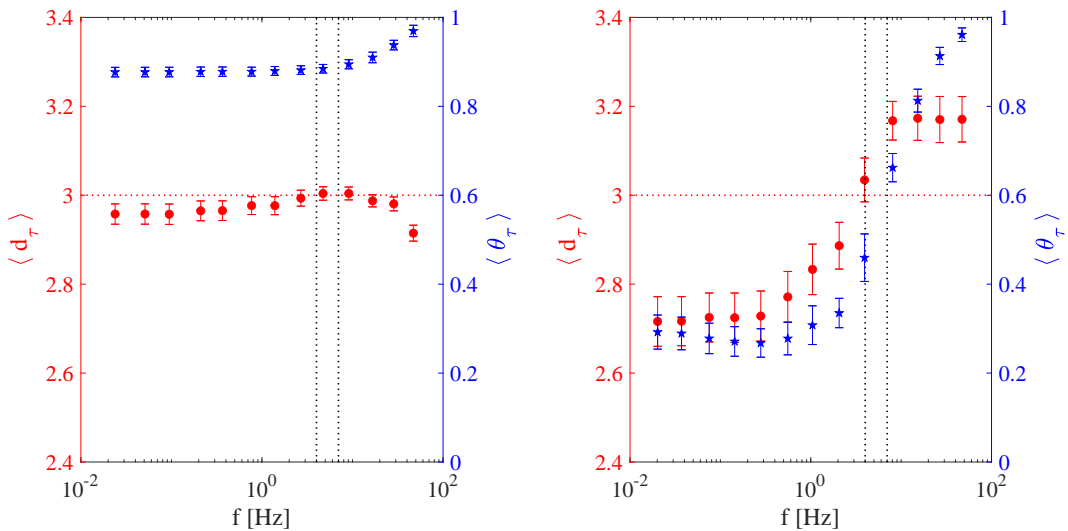


FIG. 3. Average dimension $\langle d_\tau \rangle$ (red circles) and stability indicator inverse persistence $\langle \theta_\tau \rangle$ (blue stars) as a function of the mean frequency $f = 1/\tau$. Error bars indicate the standard deviations of the instantaneous values of d_τ and θ_τ , respectively. The horizontal red line refers to the values $\langle d_\tau \rangle = 3$, while the two vertical black dashed lines correspond to $f_{s1} \sim 4$ Hz and $f_{s2} \sim 7$ Hz, respectively (see [25]). Left: $\gamma = -0.0081$, right: $\gamma = -0.0682$

Chameleon attractor The dynamical system metrics can finally be used to uncover the scale-specific properties of the topology of the chameleon attractor underlying the dynamics. To start with, we first reconstruct the attractor at a given scale using a Poincaré section obtained by plotting $\Theta_3^f(t)$ as a function of $\Theta_2^f(t)$ and $\Theta_1^f(t)$, where $\Theta_\mu^f(t)$ is the reconstruction of modes with mean frequencies $f_k > f$, with $f_k = 1/\tau_k$ as in Eq. (2). Figure 4 shows the attractor for the two limiting cases discussed previously, while the other cases are again reported in the supplementary material. We use a color scheme based on either the local dimension (upper two rows) or the instantaneous persistence (lower two rows).

In the symmetric case, $\gamma = -0.0081$, one observes that the local dimension and the inverse persistence are homogeneously distributed across the attractor, implying that its topology is very simple and can be associated with a

noisy fixed point. By contrast, the non-symmetric case attractor displays scale-dependent features with a heterogeneous spatial distribution of the two metrics.

Discussion Figure 2 (right) summarizes the strikingly different behavior of the dynamics above and below the timescale corresponding to $f = 6$ Hz, resulting in a change of the topological properties of the underlying attractor. This timescale corresponds to the natural characteristic forcing scale, thus suggesting that we observe a time behavior mirroring the well-known scaling behavior of a 3-D turbulent flow. At scales larger than the injection scale, the energy transfer is small, and the individual scales are in quasi-equilibrium; for scales smaller than the forcing scale, the mean energy transfer is positive, and there is an out-of equilibrium energy cascade towards smaller scales, following a Kolmogorov spectrum with intermittency corrections.

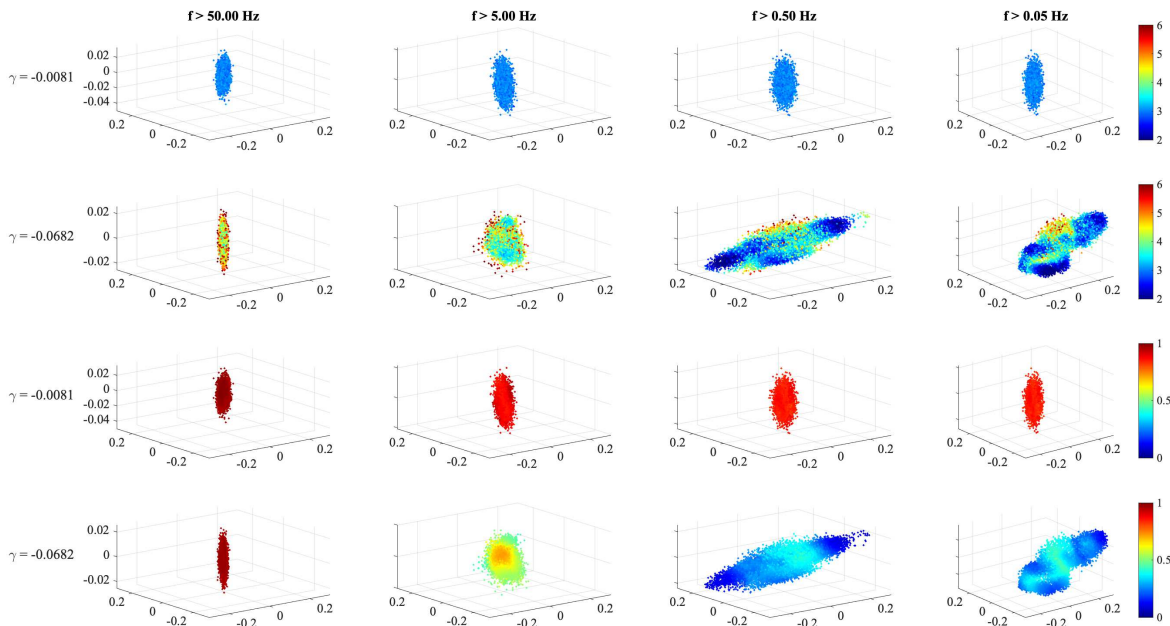


FIG. 4. 3-D attractor of the system for the two values of γ at different frequencies, colored by either the instantaneous local dimension (upper two rows) or the instantaneous inverse persistence (lower two rows). Moving from left to right we consider from high to low frequencies.

In the present case, the low frequencies are associated to dynamics in lower dimensions, showing that the statistical equilibrium at large scales is driven by a few degrees of freedom, generating a well defined low-dimensional attractor. On the other hand, the dynamics at scales smaller than the forcing effectively plays the role of noise, which restores the broken symmetry and provides the "statistical temperature" for large scales, or the stochasticity of the attractor [27].

More generally, our results demonstrate that we cannot appropriately describe such attractors with averaged properties, and that we need refined analysis tools to detect their heterogeneity and the state-dependent properties of the system. Hence, it is apparent that the analysis of multiscale systems requires considering concepts allowing us to explore local and instantaneous properties of the

system [25, 36]. Our analysis shows that the highly heterogeneous *chameleon* attractors discussed here could be common in high-dimensional dynamical systems as those encountered in climate sciences. We are confident that follow-up studies will further demonstrate their existence in such systems by exploiting the framework applied in the present work.

ACKNOWLEDGMENTS

This work was funded through ANR EXPLOIT, grant agreement no. ANR-16-CE06-0006-01 and ANR TILT grant agreement no. ANR-20-CE30-0035. VL acknowledges the support received from the EPSRC project EP/T018178/1 and from the EU Horizon 2020 project TiPES (Grant no. 820970).

-
- [1] B. Dubrulle, Beyond Kolmogorov cascades, *Journal of Fluid Mechanics* **867**, P1 (2019).
 - [2] R. Esposito, J. L. Lebowitz, and R. Marra, On the derivation of hydrodynamics from the boltzmann equation, *Physics of Fluids* **11**, 2354 (1999), <https://doi.org/10.1063/1.870097>.
 - [3] C. Foias, O. Manley, R. M. S. Rosa, and R. Temam, *Navier-Stokes Equations and Turbulence* (2001).
 - [4] A. Kolmogorov, The Local Structure of Turbulence in Incompressible Viscous Fluid for Very Large Reynolds' Numbers, *Akademiia Nauk SSSR Doklady* **30**, 301 (1941).
 - [5] R. Klein, Scale-dependent models for atmospheric flows, *Annual Review of Fluid Mechanics* **42**, 249 (2010), <https://doi.org/10.1146/annurev-fluid-121108-145537>.
 - [6] J. Berner, U. Achatz, L. Batté, L. Bengtsson, A. d. l. Cámara, H. M. Christensen, M. Colangeli, D. R. B.

- Coleman, D. Crommelin, S. I. Dolaptchiev, C. L. E. Franzke, P. Friederichs, P. Imkeller, H. Järvinen, S. Juricke, V. Kitsios, F. Lott, V. Lucarini, S. Mahajan, T. N. Palmer, C. Penland, M. Sakradzija, J.-S. von Storch, A. Weisheimer, M. Weniger, P. D. Williams, and J.-I. Yano, Stochastic Parameterization: Toward a New View of Weather and Climate Models, *Bulletin of the American Meteorological Society* **98**, 565 (2017), arXiv:1510.08682 [physics.ao-ph].
- [7] M. Ghil and V. Lucarini, The physics of climate variability and climate change, *Reviews of Modern Physics* **92**, 035002 (2020).
- [8] G. Parisi and U. Frisch, *Turbulence and predictability in geophysical fluid dynamics and climate dynamics* (North-Holland Publ. Co., Amsterdam/New York, 1985) p. 449.
- [9] A. Crisanti, M. H. Jensen, A. Vulpiani, and G. Paladin, Intermittency and predictability in turbulence, *Physical Review Letters* **70**, 166 (1993).
- [10] R. S. Ellis, The theory of large deviations: from Boltzmann’s 1877 calculation to equilibrium macrostates in 2D turbulence, *Physica D: Nonlinear Phenomena* **133**, 106 (1999).
- [11] R. Benzi, G. Paladin, A. Vulpiani, and G. Parisi, On the multifractal nature of fully developed turbulence and chaotic systems, *Journal of Physics A: Mathematical General* **17**, 3521 (1984).
- [12] U. Frisch, *Turbulence* (1995).
- [13] G. Boffetta, A. Mazzino, and A. Vulpiani, TOPICAL REVIEW: Twenty-five years of multifractals in fully developed turbulence: a tribute to Giovanni Paladin, *Journal of Physics A: Mathematical General* **41**, 363001 (2008), arXiv:0809.0196 [nlin.CD].
- [14] A. Arneodo, G. Grasseau, and M. Holschneider, Wavelet transform of multifractals, *Physical Review Letters* **61**, 2281 (1988).
- [15] J. F. Muzy, E. Bacry, and A. Arneodo, Wavelets and multifractal formalism for singular signals: Application to turbulence data, *Physical Review Letters* **67**, 3515 (1991).
- [16] R. Benzi, L. Biferale, G. Paladin, A. Vulpiani, and M. Vergassola, Multifractality in the statistics of the velocity gradients in turbulence, *Physical Review Letters* **67**, 2299 (1991).
- [17] L. Biferale, G. Boffetta, A. Celani, B. J. Devenish, A. Lanotte, and F. Toschi, Multifractal Statistics of Lagrangian Velocity and Acceleration in Turbulence, *Physical Review Letters* **93**, 064502 (2004), arXiv:nlin/0403020 [nlin.CD].
- [18] R. Benzi, L. Biferale, R. T. Fisher, L. P. Kadanoff, D. Q. Lamb, and F. Toschi, Intermittency and Universality in Fully Developed Inviscid and Weakly Compressible Turbulent Flows, *Physical Review Letters* **100**, 234503 (2008), arXiv:0709.3073 [nlin.CD].
- [19] A. Arnèodo, R. Benzi, J. Berg, L. Biferale, E. Bodenschatz, A. Busse, E. Calzavarini, B. Castaing, M. Cencini, L. Chevillard, R. T. Fisher, R. Grauer, H. Homann, D. Lamb, A. S. Lanotte, E. Lévêque, B. Lüthi, J. Mann, N. Mordant, W. C. Müller, S. Ott, N. T. Ouellette, J. F. Pinton, S. B. Pope, S. G. Roux, F. Toschi, H. Xu, and P. K. Yeung, Universal Intermittent Properties of Particle Trajectories in Highly Turbulent Flows, *Physical Review Letters* **100**, 254504 (2008), arXiv:0802.3776 [nlin.CD].
- [20] A. S. Lanotte, R. Benzi, S. K. Malapaka, F. Toschi, and L. Biferale, Turbulence on a Fractal Fourier Set, *Physical Review Letters* **115**, 264502 (2015), arXiv:1505.07984 [physics.flu-dyn].
- [21] E. N. Lorenz, Deterministic Nonperiodic Flow., *Journal of Atmospheric Sciences* **20**, 130 (1963).
- [22] D. Ruelle and F. Takens, On the nature of turbulence, *Communications in Mathematical Physics* **23**, 343 (1971).
- [23] V. Lucarini, D. Faranda, A. C. G. M. M. de Freitas, J. M. M. de Freitas, M. Holland, T. Kuna, M. Nicol, M. Todd, and S. Vaienti, *Extremes and Recurrence in Dynamical Systems* (Wiley, New York, 2016).
- [24] V. Lucarini and A. Gritsun, A new mathematical framework for atmospheric blocking events, *Climate Dynamics* **54**, 575 (2020).
- [25] D. Faranda, Y. Sato, B. Saint-Michel, C. Wiertel, V. Padilla, B. Dubrulle, and F. Daviaud, Stochastic chaos in a turbulent swirling flow, *Physical Review Letters* **119**, 014502 (2017).
- [26] S. Vannitsem and V. Lucarini, Statistical and dynamical properties of covariant lyapunov vectors in a coupled atmosphere-ocean model—multiscale effects, geometric degeneracy, and error dynamics, *Journal of Physics A: Mathematical General* **49**, 224001 (2016), arXiv:1510.00298 [physics.ao-ph].
- [27] S. Thalabard, B. Dubrulle, and F. Bouchet, Statistical mechanics of the 3d axisymmetric euler equations in a taylor–couette geometry, *Journal of Statistical Mechanics: Theory and Experiment* **2014**, P01005 (2014).
- [28] B. Saint-Michel, B. Dubrulle, L. Marié, F. Ravelet, and F. Daviaud, Evidence for forcing-dependent steady states in a turbulent swirling flow, *Physical Review Letters* **111**, 234502 (2013).
- [29] B. Saint-Michel, F. Daviaud, and B. Dubrulle, A zero-mode mechanism for spontaneous symmetry breaking in a turbulent von kármán flow, *New Journal of Physics* **16**, 013055 (2014).
- [30] F. Takens, Detecting strange attractors in turbulence, in *Lecture Notes in Mathematics, Berlin Springer Verlag*, Vol. 898 (1981) p. 366.
- [31] N. Rehman and D. P. Mandic, Multivariate empirical mode decomposition, *Proceedings of the Royal Society of London Series A* **466**, 1291 (2010).
- [32] N. R. Moloney, D. Faranda, and Y. Sato, An overview of the extremal index, *Chaos* **29**, 022101 (2019).
- [33] V. Lucarini, D. Faranda, and J. Wouters, Universal Behaviour of Extreme Value Statistics for Selected Observables of Dynamical Systems, *Journal of Statistical Physics* **147**, 63 (2012), arXiv:1110.0176 [cond-mat.stat-mech].
- [34] V. Lucarini, D. Faranda, J. Wouters, and T. Kuna, Towards a General Theory of Extremes for Observables of Chaotic Dynamical Systems, *Journal of Statistical Physics* **154**, 723 (2014), arXiv:1301.0733 [cond-mat.stat-mech].
- [35] T. Alberti, G. Consolini, P. D. Ditlevsen, R. V. Donner, and V. Quattrocioni, Multiscale measures of phase-space trajectories, *Chaos* **30**, 123116 (2020).
- [36] T. Alberti, R. V. Donner, and S. Vannitsem, Multiscale fractal dimension analysis of a reduced order model of coupled ocean-atmosphere dynamics, *Earth System Dynamics* **12**, 837 (2021).